WAKE VORTEX TRANSPORT OF ULTRAFINE PARTICLE EMISSIONS FROM THE GLIDE PATH TO THE GROUND

Frank Holzäpfel

Deutsches Zentrum für Luft- und Raumfahrt, Institut für Physik der Atmosphäre, 82234 Oberpfaffenhofen, Germany

Abstract

Ultrafine particle (UFP) emissions of aircraft may cause serious adverse health effects. The current study considers the transport of UFP emissions via the wake vortices generated by aircraft approaching Frankfurt airport down to the ground. For this purpose, the fast-time Probabilistic Two-Phase wake vortex prediction model P2P has been enhanced for the prediction of the transport of a passive tracer with the descending wake vortex oval. The study considers the year 2019 with the prevailing wind conditions and the respective traffic mix. The presented results comprise the distributions of the numbers of wake vortices reaching down to the ground and the corresponding UFP number concentrations.

1. INTRODUCTION

Besides gaseous aircraft jet emissions also aviation particulate emissions deserve attention (WHO global air quality guidelines, 2021). Within these ultrafine particles (UFP) smaller than 100 nm in diameter may cause serious adverse health effects, as they may penetrate deep into the human respiratory system. Therefore, the project "UFP-Belastungsstudie in der Region Frankfurt/Main" was launched with the mission to place the discussion about the health effects of UFP in the Rhine-Main region, and in particular the role of UFP emissions from Frankfurt Airport, on a factual scientific basis.

The current study considers the transport of the UFP emissions by the wake vortices generated by aircraft approaching Frankfurt airport along six different approach paths. For this purpose, the fast-time Probabilistic Two-Phase wake vortex prediction model P2P has been enhanced for the prediction of the transport of a passive tracer with the descending wake vortex oval, the associated turbulent mixing processes with its environment, and the detrainment into a secondary wake, all causing the dilution of the tracer on its way to the ground. The study considers the wind conditions prevailing in the year 2019 and the respective traffic mix of Frankfurt airport. The presented results comprise the number of wake vortices reaching the ground and the respective UFP number concentrations.

2. METHOD

A simulation environment has been developed in order to determine the areas where UFP may reach down to the ground by wake vortex transport and to estimate the connected UFP number concentrations.

Wake vortex transport and decay is simulated by the semiempirical fast-time Probabilistic Two-Phase wake vortex transport and decay model (P2P, Holzäpfel 2003), which considers all relevant influencing variables of the vortex generator (wingspan, weight, speed, flight path angle) as well as the environmental parameters air density, wind (crosswind and headwind), wind shear, turbulence, thermal stratification and the influence of the ground

(Holzäpfel, 2006, Holzäpfel and Steen, 2007). P2P has been validated against measurement data of four US and ten European field measurement campaigns employing over 16,000 individual cases.

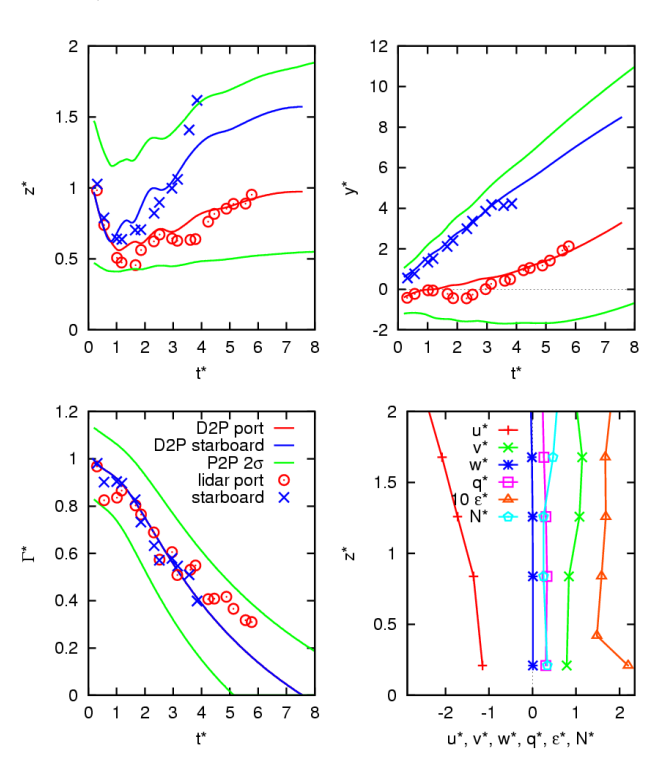


Fig. 1: Measured (symbols) and predicted (lines) wake vortex development near the ground in normalised parameters. Bottom right: Vertical profiles of the normalised meteorological parameters headwind u^* , crosswind v^* , vertical wind w^* , turbulence velocity q^* , turbulent kinetic energy dissipation rate ϵ^* and Brunt-Väisälä frequency N^* (thermal stratification).

Fig. 1 shows an example of the development of a wake vortex near the ground measured with a lidar (symbols) and predicted with P2P (lines) in dimensionless variables. The vertical position z^* and the lateral position y^* are normalised with the initial vortex spacing b_0 ; the circulation Γ^* , which is

a measure of the strength of the vortices, is normalised with its initial value, and vortex age, t^* , is normalized by the time the vortices need to descend by one vortex separation b_0 . The vortices generated at a height of about one vortex spacing above the ground initially descend due to mutual velocity induction before they rise again, driven by the interaction with the ground (top left). Due to the crosswind, the vortex behaviour becomes asymmetrical and the leeward vortex rises more strongly than the windward vortex. The influence of the ground also causes the vortices to diverge, while they experience a lateral drift driven by the crosswind (top right).

The decay of the wake vortex takes place in two phases (bottom left). The slower decay in the so-called diffusion phase changes to the rapid decay phase at $t^*=1$ due to the influence of the ground (Holzäpfel and Steen, 2007). The onset of rapid decay is controlled by the parameter T_2^* and the decay rate by an effective viscosity v_2^* , which are determined as a function of the ambient turbulence, the thermal stratification and the influence of the ground. In the current study, the deterministic predictions marked with red and blue lines are used. The probabilistic envelopes, which are shown here for a 2- σ probability (95.4%), are used for conservative predictions of the vortex behaviour to optimise aircraft separations and are not used in this study.

The aircraft parameters for determining the initial circulation of the wake vortices, Γ_0 , and their separation, b_0 , are taken from the Base of Aircraft Data (BADA) database (BADA, 2019). BADA contains the data of all aircraft types used in the study. For the approaches to the individual runways, wake vortices are simulated starting at a distance of 12 km from the runway threshold in steps of $\Delta x = 50$ m down to the threshold, which is flown over at a height of 15 m (50 feet).

Table 1 lists the considered aircraft types with the parameters relevant to this study. The analyses were carried out for air traffic and wind conditions in 2019. The number of approaches in 2019 is taken from statistics

published by the airport (Frankfurt Airport Air Traffic Statistics, 2019). The 13 most common aircraft types account for 92.6% of aircraft movements, with the A320 family dominating with 49.6% of all approaches. Nevertheless, the proportion of aircraft in the ICAO Heavy category is relatively high at 19.9%. This is important, as the largest aircraft types also generate the longest-lived wake vortices with the greatest descent depths and therefore the largest catchment areas for UFP transport. Therefore, it is also important that the A388 is included in the traffic mix (1.7%).

The UFP numbers in the last column correspond to the number of non-volatile particles emitted in one second during the approach. They were kindly provided by the Institute of Environmental Engineering (IfU) at ETH Zurich (Zhang et al. 2020).

A wind climatology for the year 2019 is used to compute the transport of wake vortices by the wind. For each class of the wind climatology, wake vortex forecasts are carried out with the respective strength and direction of the wind and the forecasts are weighted with the probability of the respective wind class. For wind classes that exceed a tailwind of 5 kts for a given runway, approaches are typically no longer carried out, so that they are not taken into account here either. To extrapolate the wind to other heights above ground, the logarithmic wind profile with a ground roughness of 0.05 m is used, which represents a cultivated landscape with very few buildings and trees.

Until now, the transport of emissions by wake vortices was not included in the P2P model. High-resolution large eddy simulations (LES) of the transport of passive tracers by wake vortices in various environmental conditions conducted by Misaka et al. (2012) are used to parameterise the UFP transport with P2P. On the length and time scales relevant for wake vortices, it can be assumed that the tiny UFP particles are transported in a good approximation like a passive tracer and mixed with the environment.

Table 1: Aircraft types considered, sorted by number of approaches with relevant parameters (ICAO: International Civil Aviation Organization, MTOW: maximum take-off weight, MLW: maximum landing weight, WV: wake vortex).

aircraft type	ICAO weight class	approaches	MTOW [kg]	MLW [kg]	span [m]	airspeed [m/s]	cirkulation [m²/s]	WV-time- scale [s]	descent distance [m]	UFP [1/s]
A320	Medium	132,977	77,000	64,500	34.1	66.9	265	17.0	205	$3.055 \cdot 10^{14}$
A321	Medium	79,356	83,000	73,500	34.1	68.6	294	15.3	205	$1.704 \cdot 10^{15}$
A319	Medium	42,543	70,000	61,000	34.1	62.7	267	16.9	205	$3.077 \cdot 10^{14}$
B738	Medium	40,248	78,300	65,310	34.3	70.5	253	18.0	208	$3.008 \cdot 10^{14}$
CRJ9	Medium	39,173	38,000	34,065	24.9	67.1	191	12.5	116	$1.185 \cdot 10^{12}$
E190	Medium	38,764	51,800	44,000	28.7	67.0	214	14.9	153	$2.954 \cdot 10^{14}$
B773	Heavy	25,028	299,300	237,680	60.9	73.0	500	28.8	467	$9.595 \cdot 10^{14}$
B748	Heavy	22,847	442,250	312,072	68.4	75.2	568	31.9	533	$9.674 \cdot 10^{14}$
A333	Heavy	15,647	212,000	179,000	60.3	66.3	419	33.6	459	$1.401 \cdot 10^{15}$
A343	Heavy	11,223	276,500	190,000	60.3	63.6	464	30.4	459	$7.812 \cdot 10^{14}$
B763	Heavy	10,585	186,880	145,150	47.6	73.1	391	22.4	341	$8.158 \cdot 10^{14}$
A388	Super	8,929	560,000	386,000	79.8	67.3	673	36.7	609	$6.010 \cdot 10^{15}$
B789	Heavy	8,420	250,830	192,777	60.1	76.8	391	35.8	457	$9.486 \cdot 10^{14}$

©2025 2

The LES elucidate that the tracer descends with the vortex oval but is also partly detrained from the oval forming a secondary wake that can extend up to the flight level. It is remarkable how strongly the decrease in tracer concentration in the vortex oval correlates with the circulation decay of the wake vortices.

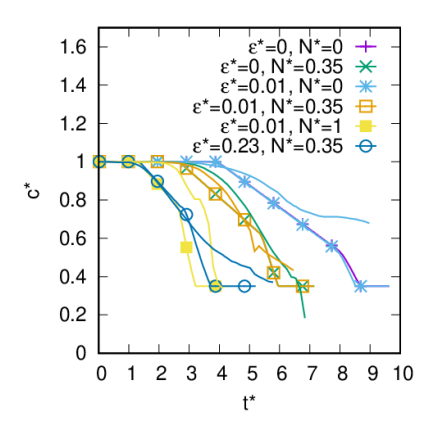


Fig. 2: Tracer concentration curve from the LES (lines) and corresponding P2P parameterisation (lines with symbols) for different environmental conditions.

Fig. 2 compares the temporal development of the passive tracer from the LES with the parameterisation developed for the P2P model. The agreement between the tracer concentration curves of the LES and the P2P parameterisation is particularly good for the most frequent average weather situation at Frankfurt Airport, with weak stable stratification with a Brunt-Väisälä frequency of N* = 0.35 (Frech et al. 2007) paired with weak atmospheric turbulence of ϵ^* = 0.01.

As soon as a wake reaches the ground, the respective number of particles is assigned to the respective ground segment. A wake vortex has reached the ground when it has descended below a height of $z=0.9\ b_0$ above the ground. This corresponds to the height at which the vortex oval, which theoretically has a vertical dimension of 1.73 b₀ (Greene 1986), approximately touches the ground. Note that the study only considers the UFP transport over the lifetime of the generated wake vortices. The further drift of the particles by the wind after the disintegration of the wake vortices is not considered.

3. WAKE VORTEX CATCHMENT AREA

Fig. 3 shows the area in which the wake vortices generated by a B773 approaching runway 07R descend to a height of at least $z=0.9\ b_0$ above ground with the winds prevailing in the year 2019. The runway threshold lies at the origin of the coordinate system and is labelled with a + symbol.

The number of wake vortex ground hits is shown in a 50 m x 50 m grid. The wake vortex is transported by the winds of all 720 classes of wind speed and direction and the ground hits are weighted with the respective frequency of the wind class. Hits from both the port and starboard vortices are counted. The area with the most hits extends along the extended runway centre line and reaches a maximum of almost 53 ground hits. As the P2P model works with a time step of one second, one hit is counted for every second that a vortex remains in a 50 m x 50 m field.

This means that the number of hits can also be interpreted as the dwell time of the two vortices in seconds over a 50 m x 50 m field at a height of less than 0.9 b₀. Fig. 1 top left illustrates that the residence time below 0.9 b₀ during the interaction of the vortices with the ground can be several characteristic time scales t_0 (cf. Table 1).

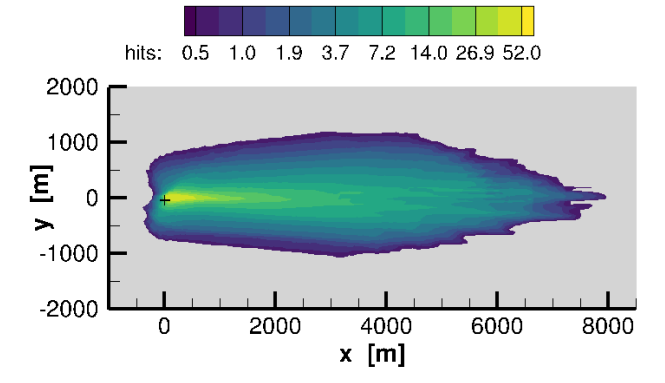


Fig. 3: Area in which wake vortices of a B773 approaching runway 07R at Frankfurt Airport can reach the ground (number of ground hits).

The area of wake vortex hits in Fig. 3 is limited to 1% of the maximum number of hits. It extends up to a distance of 7900 m from the landing threshold in the opposite direction to the approach direction. There, the flight altitude is approximately 440 m, which almost corresponds to the maximum descent depth of the B773 vortex of 467 m (see Table 1). The largest lateral dimensions are -1070 m < y < 1170 m.

4. UFP IMMISSIONS

To initialise the calculation of the UFP transport, the UFP emissions from Table 1 are used and converted into emissions per 50 m segment using the current airspeed. Fig. 4 documents the UFP number distribution on the ground caused by the wake vortices of a B773 on approach to runway 07R on an annual average. The maximum UFP number is $4.42\cdot10^{14}$, which corresponds to 67% of the emissions per second (per 50 m segment). The 1% area extends against the direction of flight almost up to x = 8000 m and in lateral direction between -1260 m and 1440 m.

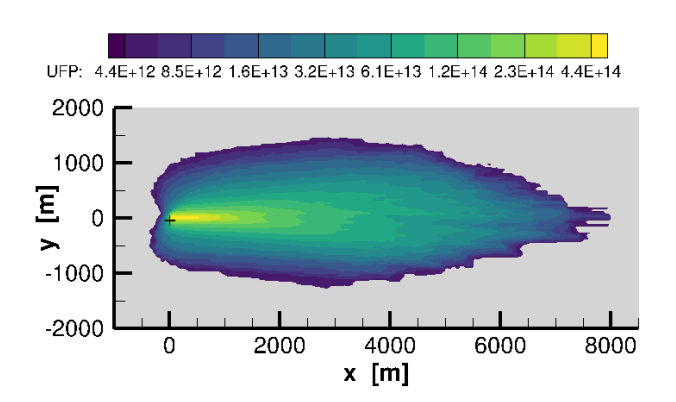


Fig. 4: UFP number distribution on the ground caused by the wake vortices of a B773 approaching runway 07R at Frankfurt Airport.

©2025 3

The next step is to calculate the UFP distributions on the ground caused by the entire traffic mix under consideration of all three runway approaches 07R, 07M, and 07L. These calculations provide an overall view of the UFP emissions and allow the relative UFP impact under the different glide paths to be compared. However, due to the weighting of the individual glide paths with the runway utilisation, the UFP values determined do not correspond to the average immissions on the ground.

Fig. 5 shows the UFP areas for approach direction 07. The maximum UFP number is 5.96·10¹³. Fig. 5 shows UFP numbers for the towns of Rüsselsheim, Raunheim and Flörsheim, whereby the part of the development exposed to the highest UFP number is selected in each case (white + symbols). These maximum values reside between 2% and 4.5% of the maximum UFP number calculated on the ground.

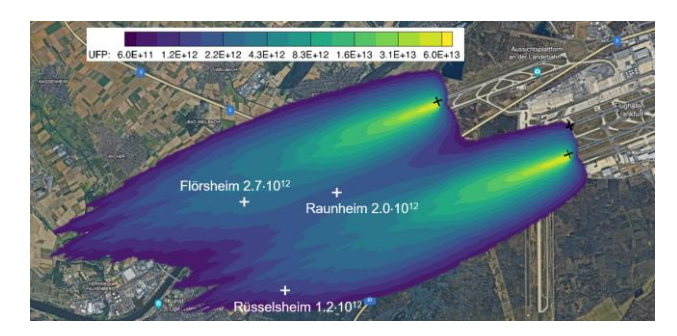


Fig. 5: UFP number distribution on the ground caused by wake vortices of the entire traffic mix in 2019 for approach direction 07 (© Google 2024).

A comprehensive description of this study will be submitted for publication to the Journal Atmospheric Environment. The introduction of the employed method will comprise a detailed description of the parametrization of the passive tracer transport. The results will encompass the distributions of wake vortices, passive tracer and UFP number concentrations for various scenarios and both runway directions. The computed UFP number concentrations will be set into perspective to the UFP concentrations measured in the airport neighbourhood.

5. ACKNOWLEDGEMENTS

The study SOURCE FFR measurements • modelling was funded by the Umwelthaus GmbH, a wholly-owned subsidiary of the state of Hessen and office of the Forum Flughafen und Region (FFR). The provision of the non-volatile particle emission numbers of the considered aircraft types by the Institute of Environmental Engineering (IfU) at ETH Zurich is greatly acknowledged. The instructive discussions with Steffen Schmitt (Institut für Verbrennungstechnik, DLR) are highly appreciated.

6. REFERENCES

BADA, May 2019. User Manual for the Base of Aircraft Data (BADA) REVISION 3.13, EEC Technical/Scientific Report No. 19/03/18-45, EUROCONTROL, 119 pages.

Frankfurt Airport Luftverkehrsstatistik 2019, Fraport AG (UEW-MF),

https://www.fraport.com/content/dam/fraport-company/documents/investoren/finanz--und-

verkehrszahlen/luftverkehrsstatistik/luftverkehrsstatistik 2019.pdf/ jcr content/renditions/original.media_fil e.download_attachment.file/luftverkehrsstatistik_2019.pdf

Frech M., Holzäpfel F., Tafferner A., Gerz T., 2007. High-Resolution Weather Data Base for the Terminal Area of Frankfurt Airport, Journal of Applied Meteorology and Climatology, Vol. 46, No. 11, pp. 1913-1932, https://doi.org/10.1175/2007JAMC1513.1.

Greene G.C., 1986. An Approximate Model of Vortex Decay in the Atmosphere, Journal of Aircraft, Vol. 23, No. 7, pp. 566-573.

Holzäpfel, F., 2003. Probabilistic Two-Phase Wake Vortex Decay and Transport Model, Journal of Aircraft, Vol. 40, No. 2, pp. 323-331, https://doi.org/10.2514/2.3096.

Holzäpfel F., 2006. Probabilistic Two-Phase Aircraft Wake-Vortex Model: Further Development and Assessment, Journal of Aircraft, Vol. 43, No. 3, pp. 700-708, https://doi.org/10.2514/1.16798.

Holzäpfel F., Steen M., 2007. Aircraft Wake-Vortex Evolution in Ground Proximity: Analysis and Parameterization, AIAA Journal, Vol. 45, No. 1, pp. 218-227, https://doi.org/10.2514/1.23917.

Misaka, T., Holzäpfel, F., Gerz, T., Manhart, M., Schwertfirm, F., 2012. Vortex bursting, tracer transport, and decay mechanisms of a counterrotating vortex pair, Physics of Fluids, Vol.24, No. 2, pp. 25104-1 - 25104-21, https://doi.org/10.1063/1.3684990.

WHO global air quality guidelines. Particulate matter (PM2.5 and PM10), ozone, nitrogen dioxide, sulfur dioxide and carbon monoxide. Geneva: World Health Organization; 2021, https://www.who.int/publications/i/item/97892400342 28.

Zhang, X., Karl, M., Zhang, L., Wang, J., 2020. Influence of Aviation Emission on the Particle Number Concentration near Zurich Airport, Environment Science and Technology, 54, 14161–14171, https://doi.org/10.1021/acs.est.0c02249.

©2025